VII. Supplemental Materials

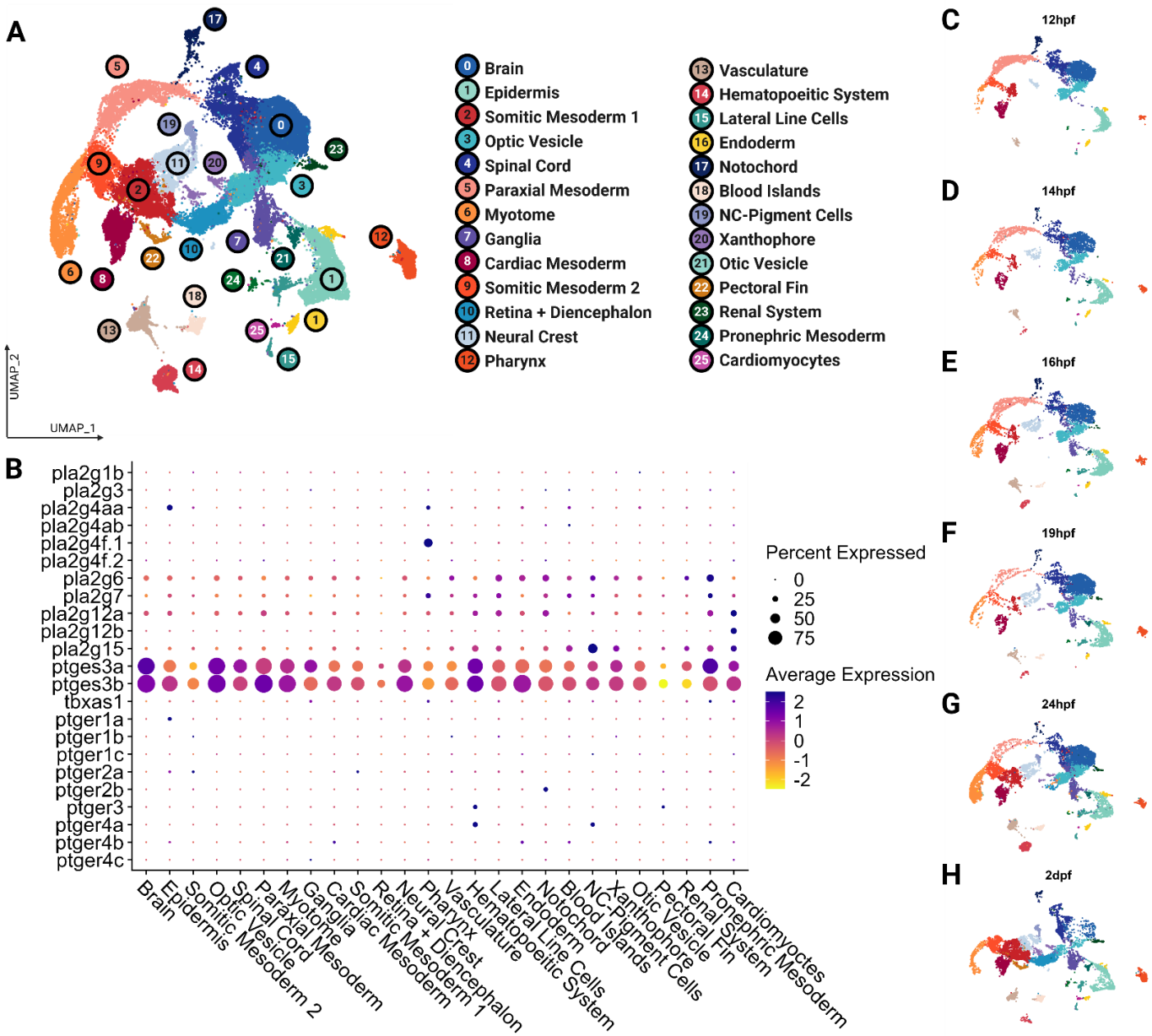

Supplemental Figure 1. Expression of cyclooxygenase enzymes across zebrafish cell types. Unsupervised clustering of publicly available scRNA-seq data of zebrafish embryos between 12hpf-2dpf demonstrates expression of cyclooxygenase enzymes. (A) UMAP demonstrating the unsupervised clustering results of zebrafish embryos. (B) Dot plot demonstrating expression levels of cyclooxygenase pathway members across zebrafish cell types. (C-H) UMAP split by stages. NC, neural crest; hpf, hours post-fertilization; dpf, days post-fertilization.

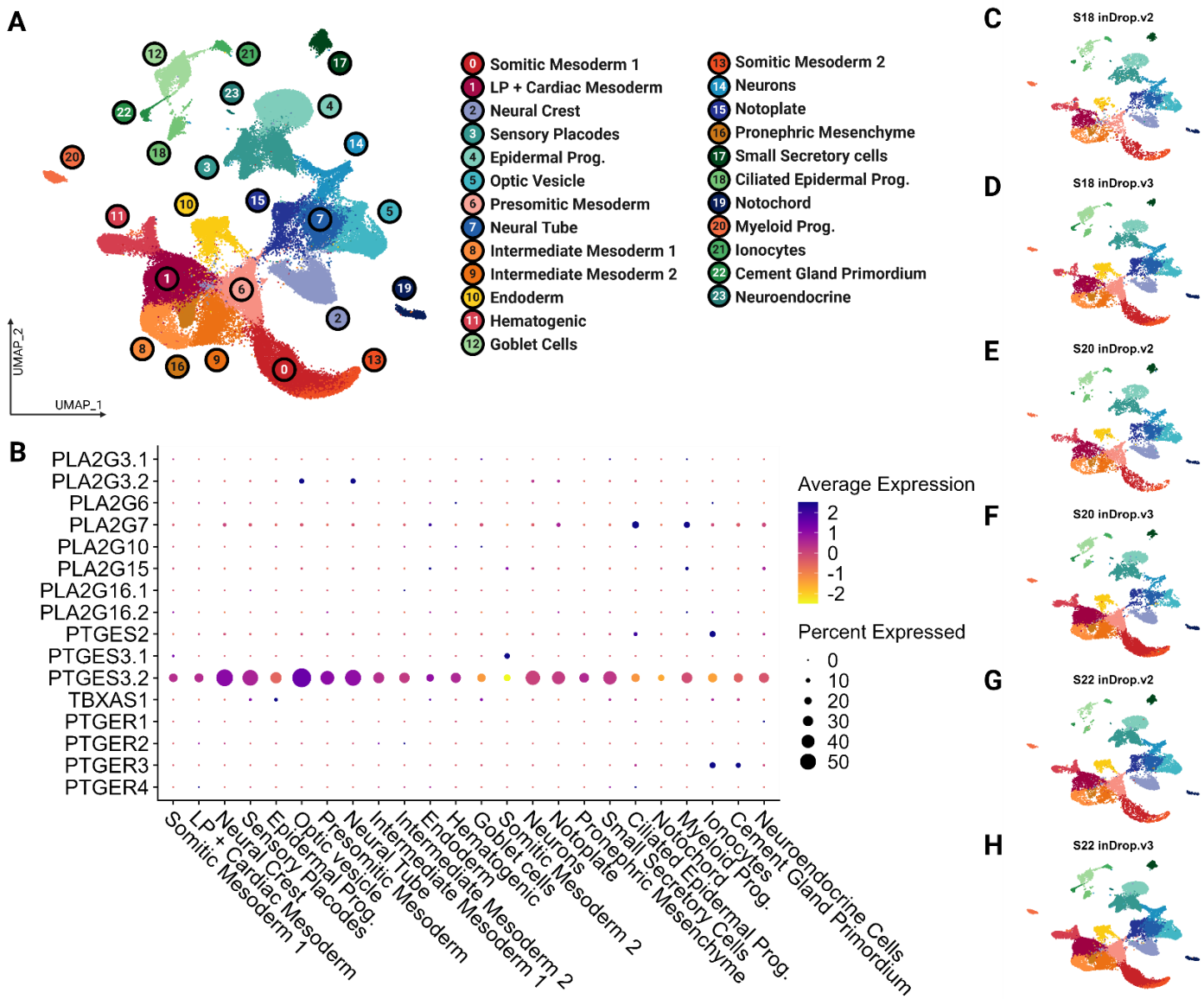

Supplemental Figure 2. Unsupervised clustering of publicly available scRNA-seq data of African clawed frog embryos between stage 18 and 22 demonstrates expression of cyclooxygenase enzymes. (A) UMAP demonstrating the unsupervised clustering results of frog embryos. (B) Dot plot demonstrating expression levels of cyclooxygenase pathway members across frog cell types. (C-H) UMAP split by stage and inDrop version. LP, lateral plate; Prog., progenitors.

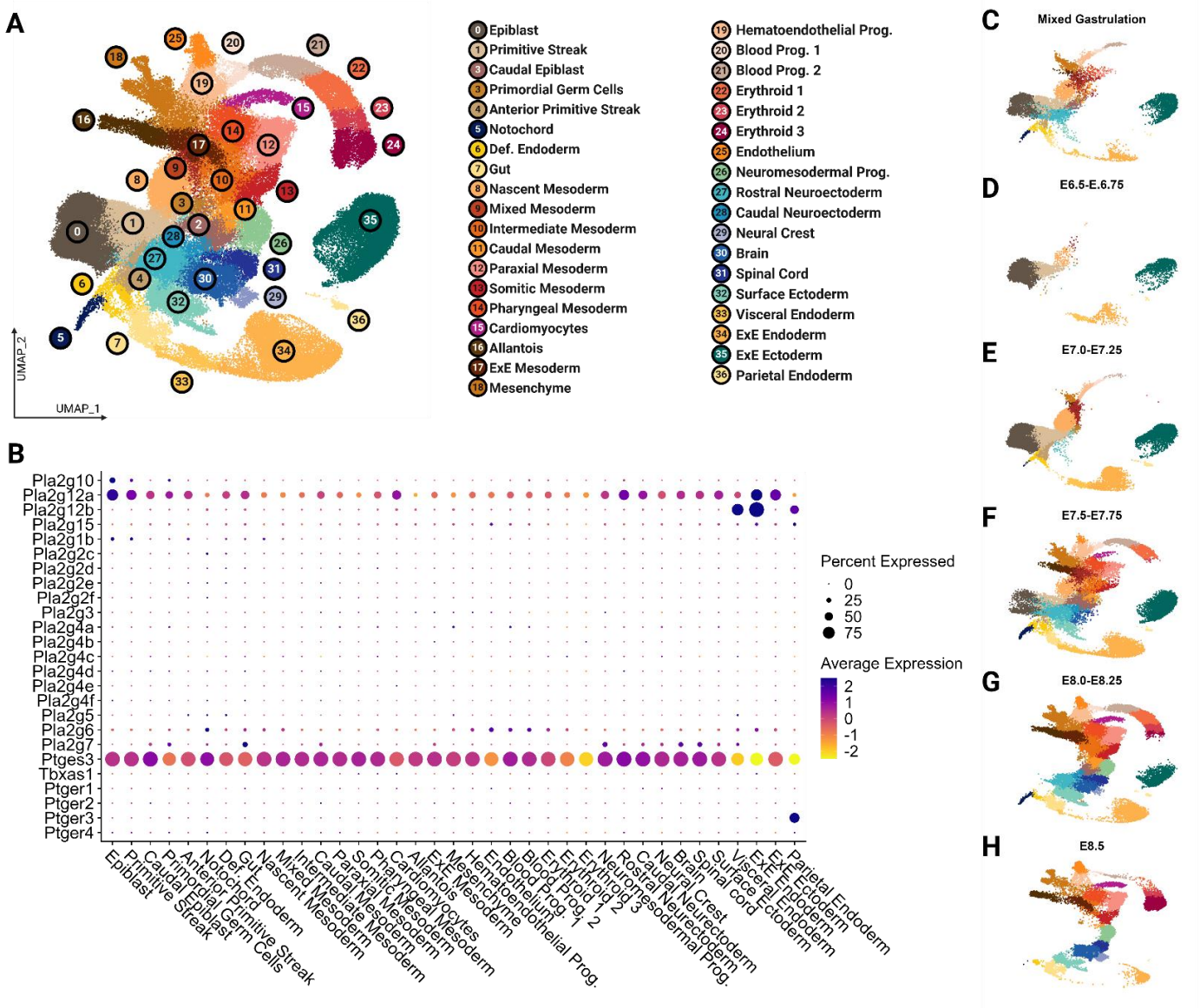

Supplemental Figure 3. Expression of cyclooxygenase enzymes across mouse cell types. Unsupervised clustering of publicly available scRNA-seq data of house mouse embryos between late gastrulation and E8.5 demonstrates expression of cyclooxygenase enzymes. (A) UMAP demonstrating the unsupervised clustering results of mouse embryos. (B) Dot plot demonstrating expression levels of cyclooxygenase pathway members across frog cell types. (C-H) UMAP split by stage. Def, definitive; Prog., progenitors; ExE, extraembryonic.

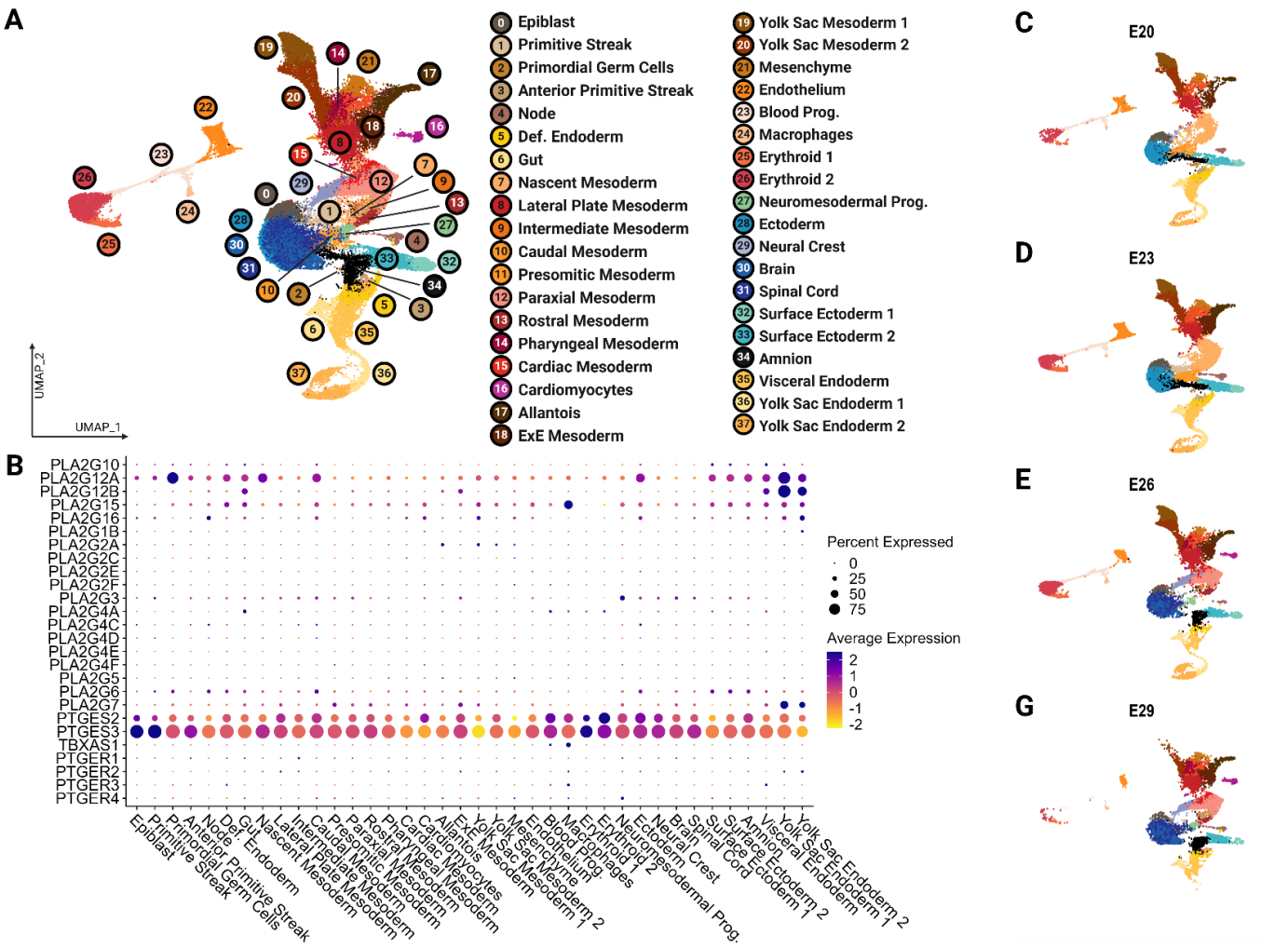

Supplemental Figure 4. Expression of cyclooxygenase enzymes across macaque cell types. Unsupervised clustering of publicly available scRNA-seq data of Cynomolgus macaque embryos between E20 and E29 demonstrates expression of cyclooxygenase enzymes. (A) UMAP demonstrating the unsupervised clustering results of macaque embryos. (B) Dot plot demonstrating expression levels of cyclooxygenase pathway members across macaque cell types. (C-H) UMAP split by stage. Def, definitive; Prog., progenitors; ExE, extraembryonic.

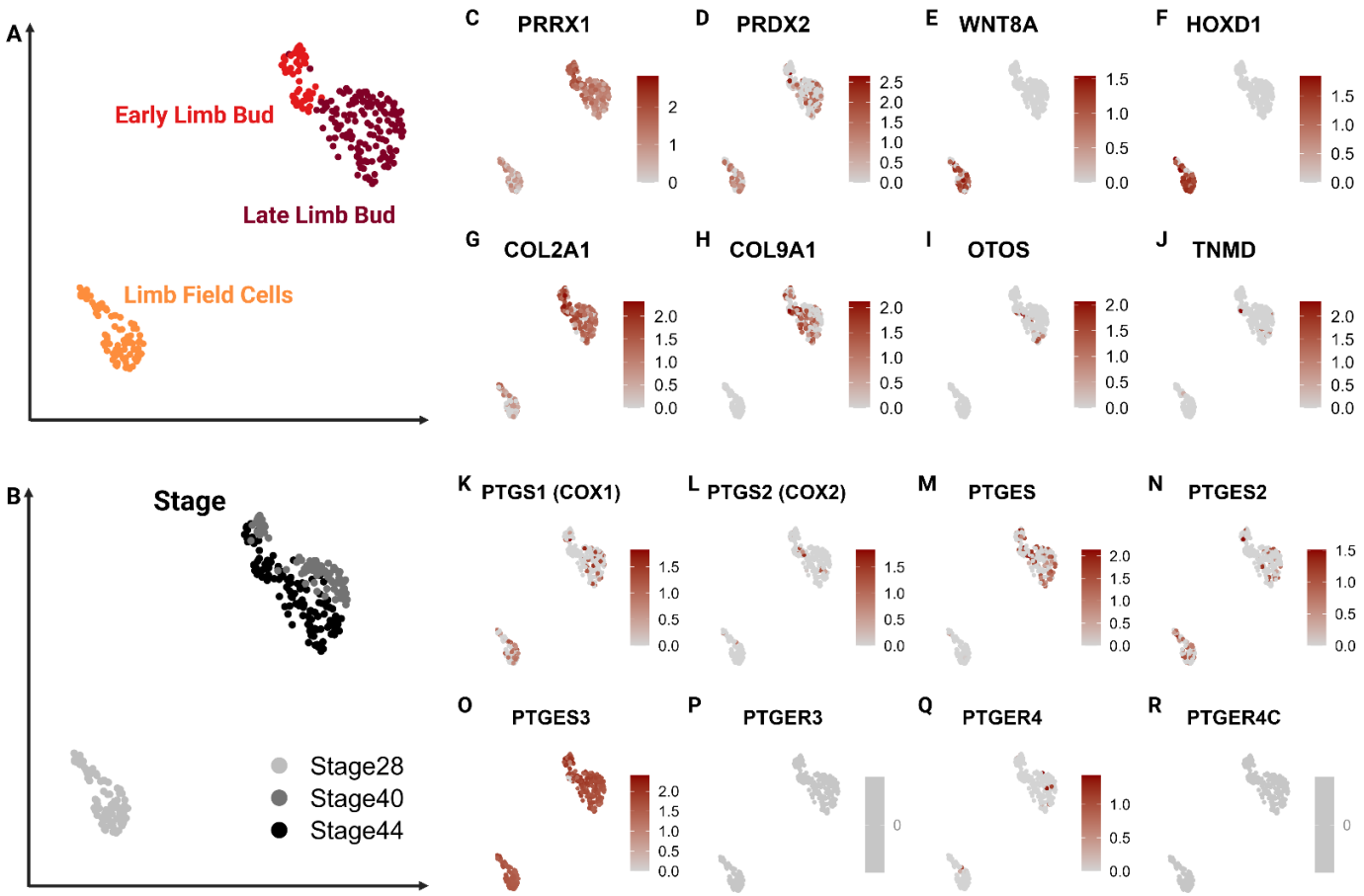

Supplemental Figure 5. Expression of cell type markers and cyclooxygenase enzymes in axolotl developing limb tissue. Unsupervised clustering of publicly available scRNA-seq data of developing axolotl limb tissue between stage 28 and stage 44 demonstrates expression of cyclooxygenase enzymes. (A) UMAP demonstrating the unsupervised clustering results of axolotl embryonic limb tissue. (B) UMAP colored by stage. (C-J) UMAP colored by expression of major marker genes. (K-R) UMAP colored by expression of cyclooxygenase pathway members.

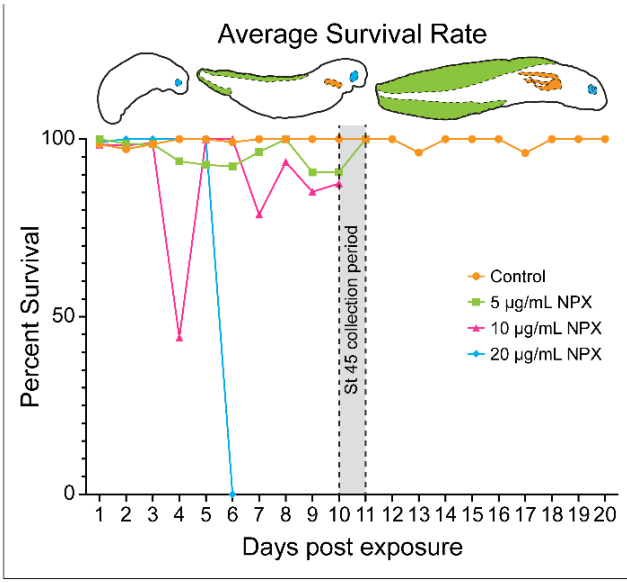

Day	Control	5 µg/mL NPX	10 µg/mL NPX	20 µg/mL NPX	Day	Control	5 µg/mL NPX
1	3 dead 208 remaining 61 collected	0 dead 292 remaining 65 collected	4 dead 266 reamining 40 collected	1 dead 115 remaining 40 collected	11	0 dead 68 remaining 13 collected	0 dead 4 remaing 4 collected
2	4 dead 143 remaining 0 collected	3 dead 224 remaining 0 collected	4 dead 222 remaining 30 collected	0 dead 75 remaining 0 collected	12	0 dead 55 remaining 0 collected	—
3	2 dead 141 remaining 0 collected	3 dead 221 remaining 0 collected	2 dead 190 remaining 6 collected	0 dead 75 remaining 0 collected	13	2 dead 53 remaining 0 collected	—
4	0 dead 141 remaining 6 collected	13 dead 208 remaining 0 collected	66 dead 118 remaining 38 collected	0 dead 75 remaining 0 collected	14	0 dead 53 remaining 0 collected	—
5	0 dead 135 remaining 11 collected	14 dead 194 remaining 40 collected	0 dead 80 remaining 40 collected	0 dead 75 remaining 40 collected	15	0 dead 53 remaining 0 collected	—
6	1 dead 123 remaining 0 collected	11 dead 143 remaining 0 collected	0 dead 40 remaining 0 collected	35 dead 0 remaining 0 collected	16	0 dead 53 remaining 0 collected	—
7	0 dead 123 remaining 0 collected	5 dead 138 remaining 9 collected	7 dead 33 remaining 0 collected	—	17	2 dead 51 remaining 0 collected	—
8	0 dead 123 remaining 0 collected	0 dead 129 remaining 0 collected	2 dead 31 remaining 0 collected	—	18	0 dead 51 remaining 2 collected	—
9	0 dead 123 remaining 0 collected	11 dead 118 reamining 0 collected	4 dead 27 remaining 0 collected	—	19	0 dead 49 remaining 37 collected	—
10	0 dead 123 remaining 55 collected	10 dead 108 remaining 104 collected	3 dead 24 remaining 24 collected	—	20	0 dead 12 remaining 12 collected	—

Supplemental Figure 6. NSAID exposure in early development reduces axolotl embryo survival in a dose-dependent manner. (Left) Embryos treated with NPX show reduced survival rate compared to control embryos. To calculate the survival rate per day the difference between the number of embryos remaining on day n and those that died between day (n-1) and day n was first calculated (# remaining - # dead). This number was then divided by the number of embryos remaining on day n and multiplied by 100 to get a percentage that survived between the two days of interest [(# remaining - # dead)/# remaining x100]. Dashed outline highlights the collection period for stage 45 embryos. Embryo drawings shown to demonstrate the normal morphological development of axolotl embryos. (Right) Numbers of embryos that were either found dead, were alive and apparently healthy, or were collected for bright-field imaging and IHC experiments based on the number of days post exposure to NPX.

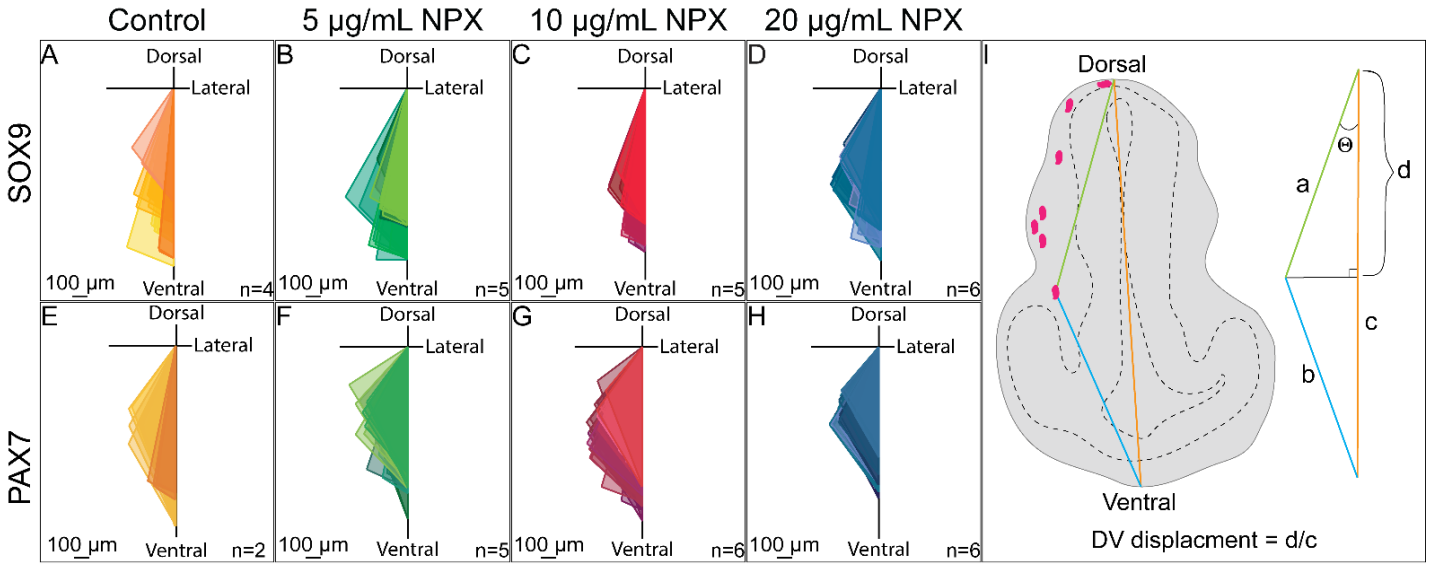

Supplemental Figure 7. Quantification of the DV displacement of SOX9/PAX7+ NC cells in the cranial region. Triangles drawn in Adobe Illustrator showing the migration patterns of (A-D) SOX9+ or (E-H) PAX7+ NC cells in transverse sections of stage 28 axolotl embryos. All triangles of the same color are from sections of the same embryo. (I) Graphical representation of a transverse section of a stage 28 axolotl embryos demonstrating the measurments and calculations used to determine the DV displacement of NC cells for each section image (quantified in Figure 4R).

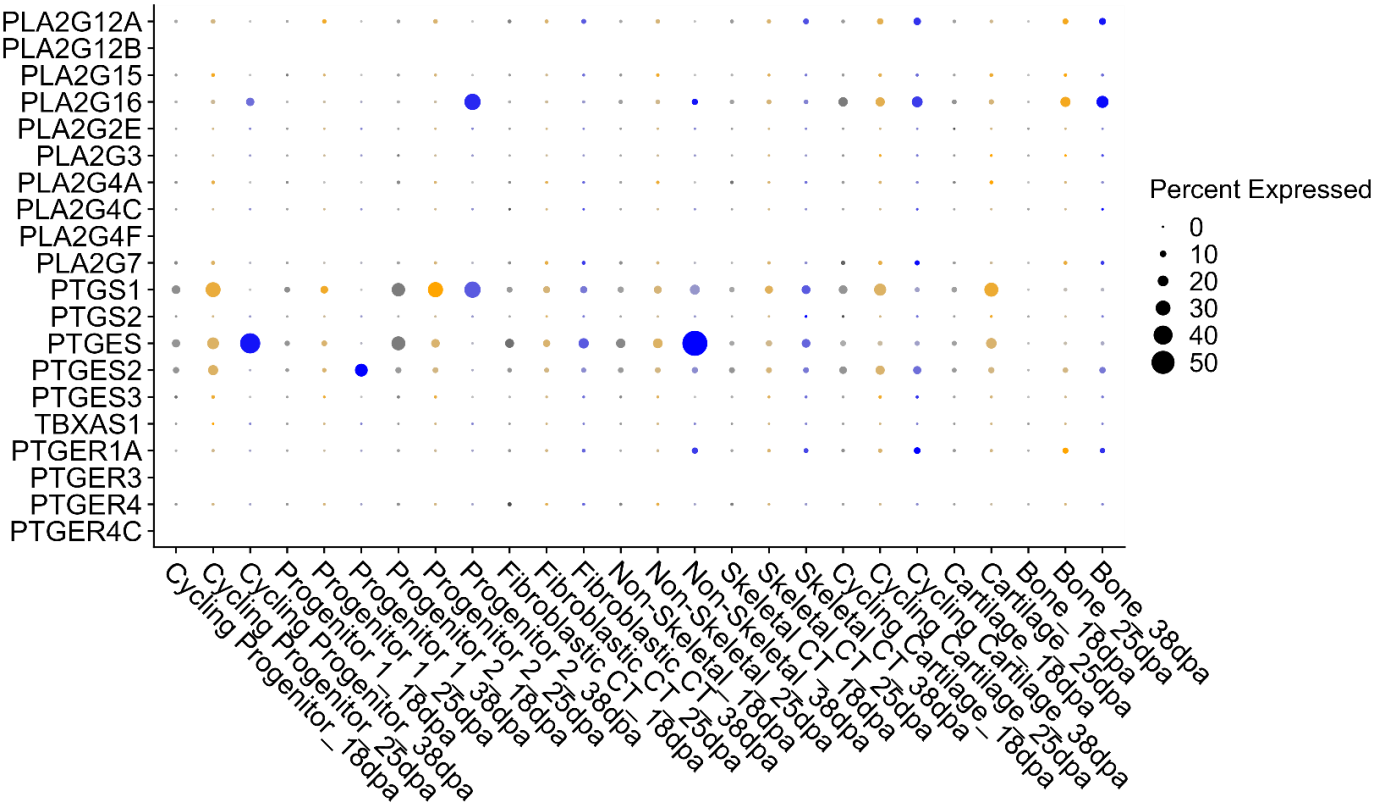

Supplemental Figure 8. Dot plot demonstrating expression of cyclooxygenase enzymes across regenerating axolotl tissue cell types split by stage. Dot plot demonstrating expression levels of cyclooxygenase pathway members across cell types identified through unsupervised clustering of regenerating axolotl limb tissue between 28 days and 38 days post amputation (dpa).

Supplementary Table 1. Methods for single cell analysis of publicly available embryonic data

Figure	Species	Data Set Features	Data Set Processing	Source
Figure 1A-G, Supp. Figure 1	*Danio rerio* (Zebrafish)	Whole embryo (12hpf, 14hpf, 16hpf, 19hpf, 24hpf, 2dpf)	Stage specific had files converted to *Seurat* v5 objects. Objects were integrated using *harmony* as per *Seurat* integration pipeline [132, 133]. Cluster annotation was determined using existing annotations from source manuscript and top marker genes of each cluster.	Datasets obtained from Zebrahub [37-40]. https://zebrahub.sf.czbiohub.org/transcriptomics
Figure 1H-N, Supp. Figure 2	*Xenopus laevis* (African clawed frog)	Whole embryo (Stage 18, 20, 22)	The count matrix and metadata files were converted to Seurat objects. Genes were renamed for analysis and can be made available on request. Objects were integrated using *harmony* as per *Seurat* integration pipeline [132, 133. Utilized 30 dimensions for reduction and 0.5 resolution for k-means clustering. Cluster annotation was determined using existing annotations from source manuscript and top marker genes of each cluster.	Datasets obtained from Tabula Rana: Xenopus Embryo Single Cell Atlas [41] https://xenopus.hms.harvard.edu/Embryo.html

{Figure 1O-U, Supp. Figure 3	*Mus musculus* (House mouse)	Whole embryo (E6.5, 6.75, E7.0, E7.25, E7.5, E7.75, E8.0, E8.25, E8.5)	The processed *SingleCellExperiment* object was downloaded via R package *MouseGastrulationData* (https://www.bioconductor.org/packages/release/data/experiment/html/MouseGastrulationData.html). Object was converted to a *Seurat* v5 object, normalized and scaled. Dimensional reduction coordinates and cell type annotations were maintained from source manuscript. Cell type colors were reassigned.	[42]
Figure 1V-AB, Supp. Figure 4	*Macaca fascicularis* (Cynomolgus monkey)	Whole embryo (CS8, CS9, CS11)	The filtered feature matrix was obtained from NCBI GEO (GSE193007) and converted to a *Seurat* v5 object, normalized and scaled. Metadata, including cell type annotation, and dimensional reduction coordinates were maintained from source manuscript. Cell type colors were reassigned.	[43]
Supp. Figure 5	*Ambystoma mexicanum* (Axolotl)	Developing limb tissue (Stage 28, 40, 44)	The processed matrix including metadata was obtained from NCBI GEO (GSE106269_Table_S7.csv) and converted to a *Seurat* v5 object and the stages of interest were subset. Object was integrated by time point using *harmony* as per *Seurat* integration pipeline [132, 133]. Utilized 11 dimensions for reduction and 0.6 resolution for k-means clustering. Cluster annotation was determined using canonical markers utilized by source manuscript.	[44]
Figure 2, Supp. Figure 8	*Ambystoma mexicanum* (Axolotl)	Limb blastema (18dpa, 25dpa, 38dpa)	The processed matrix including metadata was obtained from NCBI GEO (GSE106269_Table_S9.csv) and converted to a *Seurat* v5 object. Object was integrated by time point using *harmony* as per *Seurat* integration pipeline [132, 133]. Utilized 10 dimensions for reduction and 0.4 resolution for k-means clustering. Cluster annotation was determined using canonical markers utilized by source manuscript.	[44]